Acta Alimentaria, Vol. 46 (4), pp. 428–438 (2017)
DOI: 10.1556/066.2017.46.4.5

GREEN SYNTHESIS OF PECTIN MEDIATED HYDROXYAPATITE NANOPARTICLES FROM CULINARY BANANA BRACT AND ITS CHARACTERIZATION

Y.A. Begum and S.C. Deka*

Department of Food Engineering and Technology, Tezpur University, Assam-784 028, India

(Received: 1 September 2016; accepted: 13 February 2017)

Green synthesis of hydroxyapatite (HA) nanoparticles was followed using various concentrations of pectin extracted from the culinary banana bract. The effect of pectin concentrations on purity, crystallinity, particle size, and morphology of synthesized HA nanoparticles were studied. The extracted pectin was characterized by proton-1 nuclear magnetic resonance spectroscopy (^{1}H NMR) and Fourier transform infrared (FT-IR) spectroscopy. FT-IR results revealed that increased concentration (0–0.075 % w/w) of pectin substantially improved the purity level of synthesized HA nanoparticles. In addition, higher concentration of pectin also reduced the crystallinity and size of the synthesized HA nanoparticles, which was confirmed by X-ray diffraction (XRD) and SEM results, respectively. The synthesized HA nanoparticles at increased pectin concentration ($HA_{0.075}$) evinced high purity, less crystallinity, and discrete uniform shape. Results of TEM images have the credence to reveal the presence of nanosized discrete particles (20–50 nm) with lattice structure of hydroxyapatite.

Keywords: hydroxyapatite, template, pectin, HA nanoparticle, culinary banana bract, synthesis

Hydroxyapatite is the most attractive bioactive ceramic material and the main inorganic component of bone and human hard tissue. It has been widely used in various biomedical fields such as dental implants, alveolar bridge augmentation, orthopedics, maxillofacial surgery, scaffold materials, and drug delivery agents (Suchanek & Yoshimura, 1998). The excellent biocompatibility, bioactivity, and biodegradability of hydroxyapatite, have made its application in bone tissue engineering (Wu et al., 2013), drug delivery (Yu et al., 2014), and cell imaging (Hui et al., 2012; Zhang et al., 2013). Nanosized hydroxyapatite has raised great interests for its outperforming characteristics compared to corresponding counterparts with larger dimensions. Nanosized hydroxyapatite could exhibit unique anti-tumour ability (Tang et al., 2014). There are several synthesis methods used to generate nano-HA. However, these production methods are usually expensive, labour-intensive, and are potentially hazardous to the environment and living organisms (Narayanan & Shaktivel, 2010). Moreover, the chemicals used for the synthesis of hydroxyapatite led to the presence of some toxic substances adsorbed on the surfaces that may have adverse effects in biomedical applications (Zeng et al., 2011). Currently emphasis has been given on the use of agricultural wastes, which have the application potential in biotechnological aspect, because they are non-toxic, abundant, easily available, totally regenerable, non-exotic, cheap, and able to support rapid growth (Dhanasekaran et al., 2011). Recently, synthesis of hydroxyapatite nanoparticles was achieved using naturally available agricultural banana peel and prickly pear peel as template (Gopi et al., 2014; 2015).

* To whom correspondence should be addressed.
Phone: + 919435408396; e-mail: sankar@tezu.ernet.in

Bracts of banana are abundant residues of banana production, and 300 kg of coloured bracts per hectare are disposed as residues during harvesting of banana (Preethi & Balakrishnamurthy, 2011). However, culinary banana bract is an excellent source of anthocyanin (Begum & Deka, 2017). Banana flower contains substantial amounts of pectic polysaccharide, hemicellulose A and hemicellulose B polysaccharides (Jamuna et al., 2012). As pectin is rich in carboxyl and hydroxyl groups, it can stimulate the binding of calcium ions (Ca^{2+}) from the solution to carboxylate ions, which initiates the crystal nucleation and growth (Gilbert et al., 2005).

The present study has been focused on synthesizing HA nanoparticle using culinary banana bract pectin as template, and the influence of pectin concentration on purity, crystallinity, size, and morphology of synthesized HA nanoparticles have been studied elaborately. The method described here provides a simple, cost effective, and reliable green technology approach to synthesize HA nanoparticles as compared to chemical synthesis method. Moreover, it gives the best way of exploiting culinary banana bract and is the first attempt of synthesizing HA nanoparticles from the pectin of this agro-waste.

1. Materials and methods

1.1. Materials

Ethanol, toluene, acetone, aqueous ammonia, calcium chloride dihydrate ($CaCl_2.2H_2O$) and diammonium hydrogen phosphate ($(NH_4)_2HPO_4$) were purchased from Sigma Aldrich. All chemicals were of high purity, analytical grade.

1.2. Determination of pectin content as calcium pectate in culinary banana bract

Pectin content was determined by extraction and saponification (Ranganna, 1986) followed by precipitation as calcium pectate by calcium chloride.

1.3. Collection of sample and preparation of plant material

Culinary banana (*Musa* ABB) flowers were obtained from Tezpur University Campus, Assam. The flower was washed with distilled water, rinsed with acetone, and the bract was separated from male bud (Fig. 1). The bracts were cut into pieces and kept in oven at 60 °C for 24 h, and were ground into fine powder by using laboratory grinder.

1.4. Extraction of pectin from banana bract powder

Banana bract powder containing pectin (3.97%) was heated with 1:2 ratio of toluene-ethanol for 5 h and filtered through Whatman No.1 filter paper. The residue was extensively washed with 60% of aqueous ethanol to remove impurities, pigments, and free sugars until the filtrate was colourless. The residue was dried by solvent exchange with 95% ethanol and acetone, and finally, dried in an oven at 40 °C for 24 h.

The dried cell wall material was suspended in double distilled water (solid–liquid ratio 1:25, w/v) and the suspension was stirred at 60 °C for 4 h. The residue was resuspended in double distilled water (solid–liquid ratio 1:25, w/v), and same procedure was repeated as mentioned above. The supernatant from the second extraction was added to the first extract and mixed with four volumes of ethanol to precipitate the water soluble pectin. The obtained precipitate was filtered and dried at 40 °C and used for further experiments (Gopi et al., 2014).

Fig. 1. Culinary banana bract with male flower bud

1.5. Synthesis of HA nanoparticles

In a typical HA synthesis process, $CaCl_2.2H_2O$ and $(NH_4)_2HPO_4$ were taken as precursors for Ca and P with a molar ratio of 1.67 and dissolved in double distilled water to form 0.05 M and 0.03 M solution, respectively (Gopi et al., 2014). Various concentrations of pectin (0% w/w, 0.025% w/w, 0.05% w/w, and 0.075% w/w) was dissolved in 50 ml of double distilled water and heated to 60 °C. After that 0.05 M $CaCl_2.2H_2O$ was added to the pectin solution and stirred for 1 h to ensure the cooperative interaction and self-assembly process. Subsequently, 0.03 M $(NH_4)_2HPO_4$ solution was added drop wise into the above mixed solution under continuous and vigorous magnetic stirring for 3 h and yielded a dirty white suspension. The pH of the above suspension was maintained at 9 by using aqueous ammonia solution and stirred for 24 h. The obtained white precipitate was kept in an ultrasonicator for 1 h at 45 °C to ensure the homogeneous mixture and dried in a hot air oven at 80 °C. The dried powder was washed three times with ethanol and followed by deionized water to remove the residual pectin and chloride ions. It was then calcined for 24 h and sintered at 600 °C for 6 h. HA nanoparticles synthesized in various concentrations of pectin, viz. 0.025% w/w, 0.050% w/w, and 0.075% w/w coded as $HA_{0.025}$, $HA_{0.050}$, and $HA_{0.075}$, respectively. One set of HA nanoparticle was also synthesized without addition of pectin (control) and coded as HA_0.

1.6. Characterization techniques for pectin

1.6.1. NMR analysis. ^{1}H NMR was carried out for structural analysis of extracted pectin from the bract of culinary banana. ^{1}H NMR was performed in JNM-ECS400 spectrometer (JEOL, Japan) operating at 399.78 MHz frequency. Dry pectin sample (5 mg) was dissolved in D_2O (Acros) at 10 mg ml^{-1} concentration and the NMR spectra were recorded at 23.4 °C. The spectra were accumulated with a 4.75 μs pulse, an acquisition time of 2.18 s, a recycle time (relaxation delay) of 5 s, 8 scans and a sweep width of 7.50 kHz. ^{1}H chemical shifts were expressed in parts per million (ppm).

1.6.2. FT-IR analysis. The characterization of the extracted pectin was done using FT-IR Spectrum 100 spectrophotometer (Perkin Elmer, USA) in the region of 400–4000 cm^{-1} with 4 cm^{-1} resolution and 16 scans were collected.

1.7. Characterization of HA nanoparticles by FT-IR, XRD, SEM, and TEM

The characterization of the synthesized HA nanoparticles was done as referred in the preceding section 1.6.2.

The investigation of the phase composition and crystallinity of the synthesized HA nanoparticles was performed using Rigaku MiniFlex model (Japan) and operated at 30 kV and 15 mA. The analysis was recorded over the 2ɵ range of 10–60 °C at a scan rate of 2.0° min^{-1}. The crystallite size and crystallinity were determined based on Debye–Scherrer's equation as follows

$$X_s = \frac{0.9\lambda}{\beta \cos\Theta}; \qquad X_c = \left(\frac{0.24^3}{\beta}\right)$$

where, X_s is the crystallite size (nm), X_c is the crystallinity, λ is the wavelength of X-ray beam (λ=0.15406 nm for Cu Kα radiation), β is the full width at half maximum (FWHM) for the diffraction peak under consideration (rad). The diffraction peak at 25.80 °C was chosen for the calculation of crystallite size and crystallinity.

The structural and morphological features of the synthesized HA nanoparticles were analysed by JSM-6390LV (Jeol, Japan) scanning electron microscope. SEM was operated with 20 kV at magnification of ×20000.

The size and morphology of HA nanoparticles were further investigated by JEM-2100 (Jeol, USA) transmission electron microscope operated with 200 kV.

2. Results and discussion

2.1. ^{1}H NMR for the extracted pectin

Culinary banana bract contains 3.97 g/100 g (Table 1) pectin as calcium pectate, and NMR spectroscopy is capable of providing detailed information about the proton environment of the extracted pectin. As illustrated in Figure 2, a sharp signal at 3.67 ppm was responsible for the protons in the methoxy groups of the esterified pectin (Winning et al., 2007). The signal found around 3.7, 4, 4.6–4.8, 4.4, and 5.0 ppm corresponded to the protons of H-2, H-3, H-4, H-5 protons adjacent to the free carboxylate, and H-5 protons adjacent to the ester groups, respectively (Rosenbohm et al., 2003; Gopi et al., 2014). The entire signal in ^{1}H NMR confirmed the presence of D-galacturonic acid in the extracted material from the bract of culinary banana.

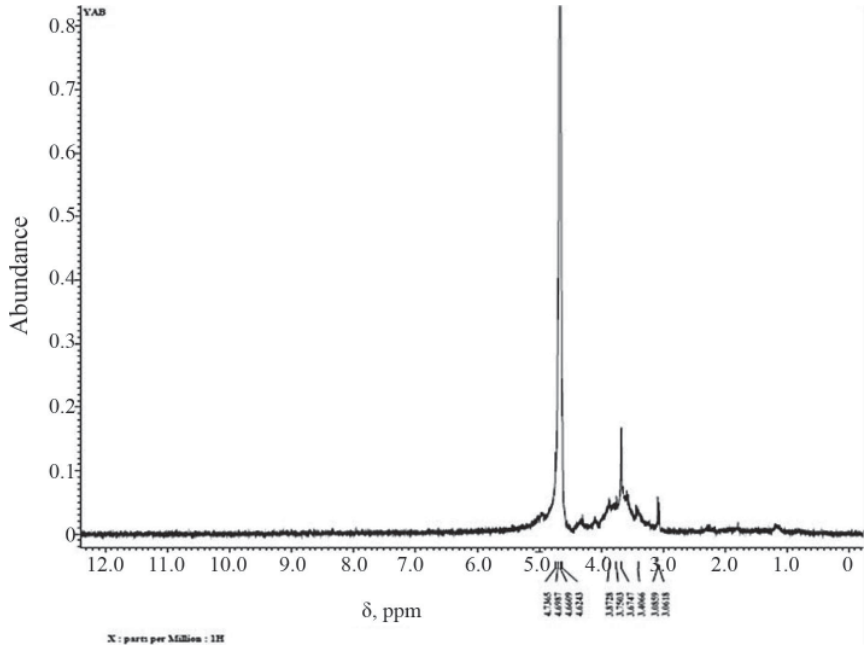

Fig. 2. ^{1}H NMR spectrum of pectin extracted from culinary banana bract

Table 1. Crystallinity of the synthesized HA nanoparticles

Pectin as calcium pectate in culinary banana bract (%)	Concentration of pectin (w/w %)	Full width half maximum (°)	Crystalline size X_s (nm)	Crystallinity X_c (%)
3.97	0	0.264	32.26	0.786
	0.025	0.290	29.36	0.565
	0.05	0.500	17.03	0.110
	0.075	0.684	12.45	0.042

2.2. FT-IR spectrum of the extracted pectin

Functional groups of pectin extracted from banana bract were identified by FT-IR, and the spectrum is presented in Figure 3. A broad peak observed at 3438 cm^{-1} and a peak found at 2929 cm^{-1} are responsible for the characteristic stretching frequency of –OH group and C–H stretching of the methyl esters of galacturonic acid (Liu et al., 2010). The absorption band at 1737 cm^{-1} and 1620 cm^{-1} was attributed to the absorption of carboxylic groups and carboxylate (Inbar et al., 1989; Chatjigakis et al., 1998). The peaks found at 1409 cm^{-1}, 1238 cm^{-1},

1108 cm^{-1}, 1016 cm^{-1}, and 950 cm^{-1} were due to the vibration of the C–O–H in plane bending, asymmetric C-O-C stretching vibration, and indicated the presence of –O–CH_3 (methoxyl) groups, bending modes of acetal, ethereal groups and glycosidic group (Gopi et al., 2014). Thus, the presence of pectin was suggested in the extracted cell wall material of banana bract by the above characteristic peaks in the spectrum.

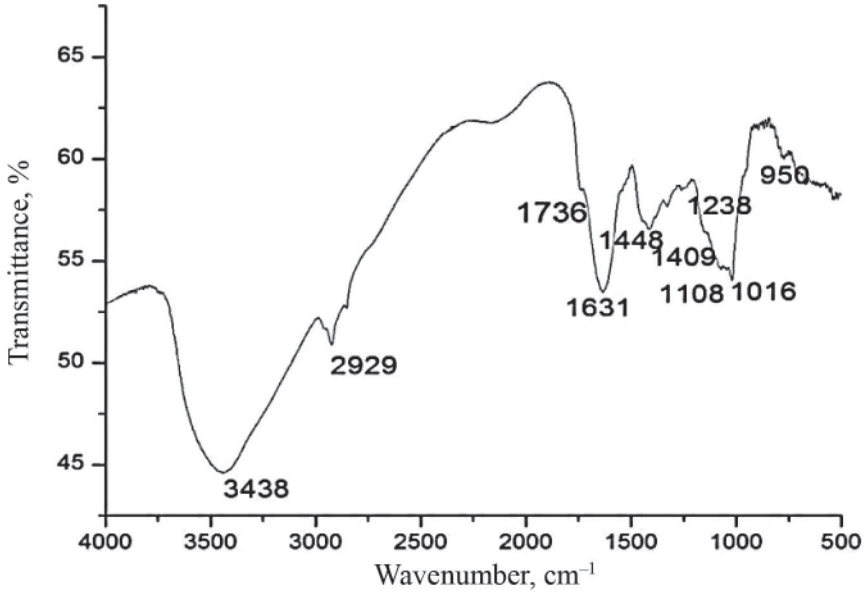

Fig. 3. FT-IR spectrum of the pectin extracted from culinary banana bract

2.3. FT-IR spectra of the synthesized HA nanoparticle

FT-IR spectra of the HA synthesized in the absence and presence of different concentrations of pectin extracted from the bract of culinary banana are shown in Figure 4A–D. The FT-IR spectrum (Fig. 4A) revealed the presence of HA along with tricalcium phosphate (TCP) in absence of pectin (Gopi et al., 2008). The characteristic peaks of hydroxyl stretching and bending vibration modes were detected at 3570, 628, 1088, 1037, and a minor peak at 960 cm^{-1} corresponded to hydroxyl stretching, bending vibration modes, and stretching vibrational modes of PO_4^{3-} (Gopi et al., 2010). The peaks resulted from the doubly degenerate bending mode of the P–O bond were found at 602 and 563 cm^{-1}, and the peak at 474 cm^{-1} resembled to the doubly degenerate bending mode of the same group (Maisara & Pat, 2011). All peaks found in this spectrum strongly confirmed the formation of HA, and the peaks were identified with improved purity as evidenced from Figure 4D at 0.075% w/w of pectin. Hence, the formation of HA preferred high concentrations of pectin.

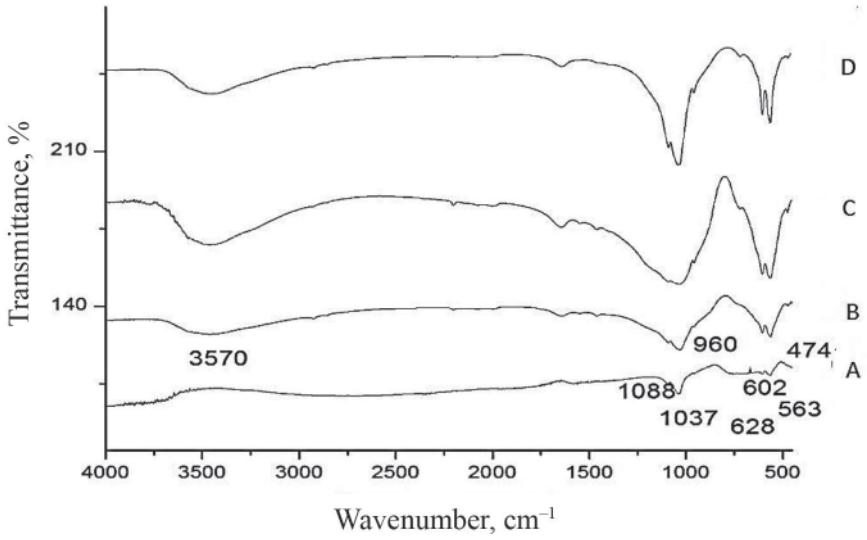

Fig. 4. FT-IR spectrum of HA nanoparticles synthesized in various concentrations of pectin (A: HA_0; B: $HA_{0.025}$; C: $HA_{0.050}$ and D: $HA_{0.075}$)

2.4. XRD patterns of the synthesized HA nanoparticles

The crystallinity of the synthesized HA nanoparticles is an important factor for its biomedical uses. The XRD patterns of synthesized HA nanoparticles in the absence and presence of different concentrations of pectin extracted from bract of culinary banana are illustrated in Figures 5A–5D. The XRD pattern of the HA nanoparticle synthesized in absence of pectin are shown in Figure 5A. The diffraction peak at 25.80 °C was an isolated sharp one and was selected for the calculation of crystallite size and crystallinity. XRD results demonstrated (Table 1) the crystallinity of 0.78% for HA nanoparticle synthesized in absence of pectin, whereas this was found to be 0.04% for the HA nanoparticles synthesized with 0.075% w/w of pectin. Gopi and co-workers (2015) also found decrease in crystallinity with increasing pectin concentration from 0.04 to 0.15 w/w %. Furthermore, by increasing the concentration of pectin to 0.2 and 0.25% w/w, crystallinity was found to increase. The reason for the lower crystallinity might be the size effect owing to the three-dimensional network microstructure provided by the cross-linked pectin molecule (Christensen, 1986). Usually, the HA with low crystalline nature is desirable for biomedical purposes due to their high in vivo resorbable property (Dorozhkin & Epple, 2002). Hence, higher concentration of pectin exhibits poor crystallinity and therefore the addition of 0.075% w/w of pectin has a significant effect on decreasing the crystalline nature of the synthesized HA nanoparticles.

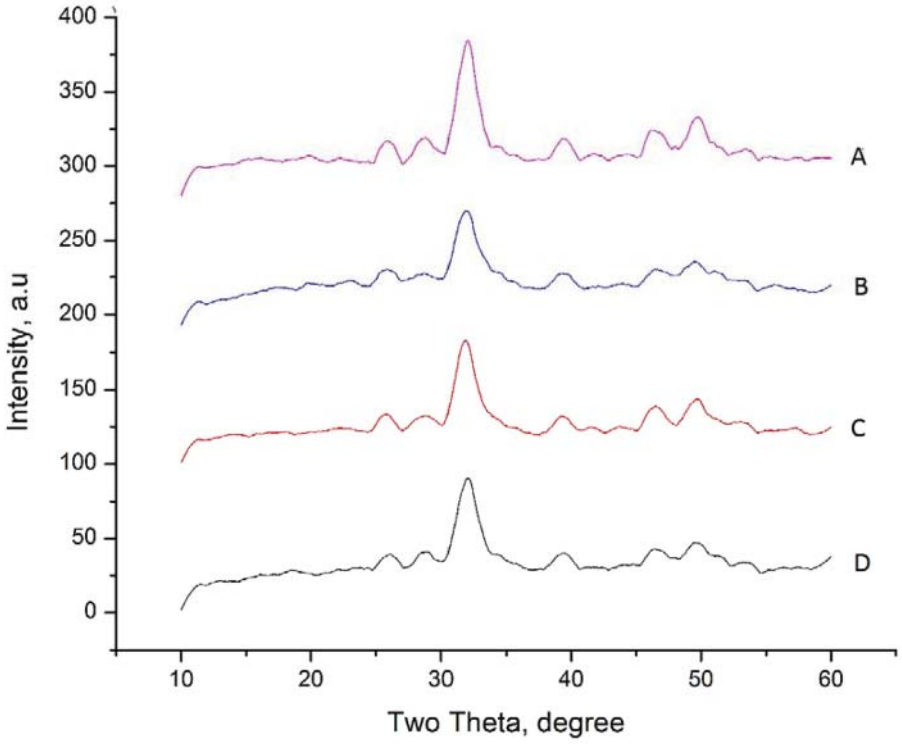

Fig. 5. XRD patterns of HA nanoparticles synthesized in various concentrations of pectin (A: HA_0; B: $HA_{0.025}$; C: $HA_{0.050}$ and D: $HA_{0.075}$)

2.5. SEM analysis of the HA nanoparticles

SEM micrographs of HA nanoparticles synthesized in the absence and presence of various concentrations of pectin are shown in Figures 6A–6D. HA nanoparticle synthesized in absence of pectin seems to be spherical and agglomerated (Fig. 6A), discrete particles were seen in the micrograph (Fig. 6B) with certain levels of agglomeration at 0.025% w/w of pectin concentration. As the pectin concentration increased to 0.05% w/w, the size of the particles decreased and the morphology seemed to be spherical (Fig. 6C). Further increase of pectin concentration to 0.075% w/w resulted smaller sized and uniform discrete spherical-like nanoparticles (Fig. 6D) with size ranges of 50–60 nm. Therefore, the optimum concentration for obtaining the uniform sized pure HA nanoparticles was 0.075% w/w. The importance of pectin concentration from banana peel in facilitating the synthesis of nanosize hydroxyapatite was shown by Gopi and co-workers (2014).

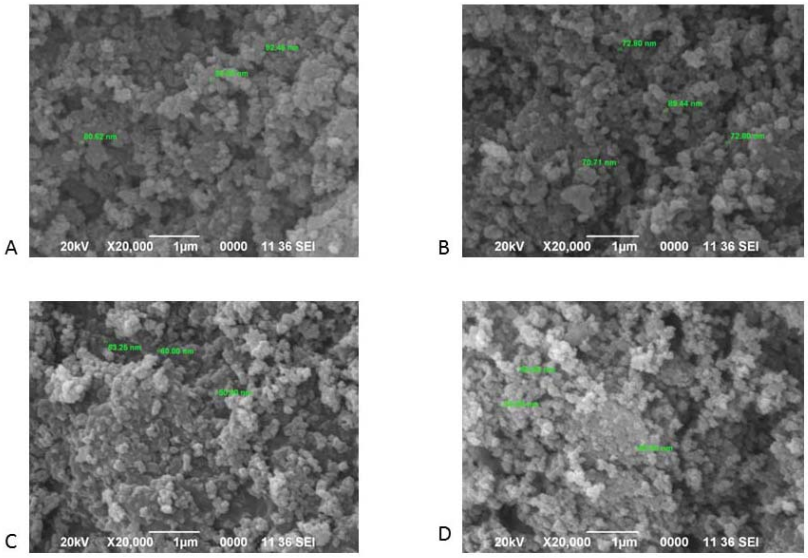

Fig. 6. SEM micrographs of HA nanoparticles synthesized various concentrations of pectin (A: HA_0; B: $HA_{0.025}$; C: $HA_{0.050}$ and D: $HA_{0.075}$)

2.6. Transmission electron microscopy (TEM) analysis of the HA nanoparticle

The results of FT-IR, XRD, and SEM revealed that HA nanoparticles with 0.075% w/w of pectin ($HA_{0.075}$) were found best in terms of purity, crystallinity, and morphology. Therefore, $HA_{0.075}$ was chosen for its size and morphology analysis by TEM, and its images are presented at various dimensions in Figures 7A–7D. $HA_{0.075}$ showed particles with the size ranged of 20 to 50 nm, which was evident from TEM micrograph. HA synthesized at the optimized concentration of pectin extracted from banana peel (0.15% w/w) showed particles with size range from 35 to 55 nm (Gopi et al., 2014).

The TEM images in Figures 7A–7C revealed that the HA particles synthesized in this study was nanosized and had irregular to spherical shape. In addition, the selected area electron diffraction (SAED) in Figure 7D of the precipitates showed the diffraction dots or rings reflect, which implies that the precipitates were crystalline in nature. The SAED results of nano HA favourably corroborate the lattice structure of hydroxyapatite.

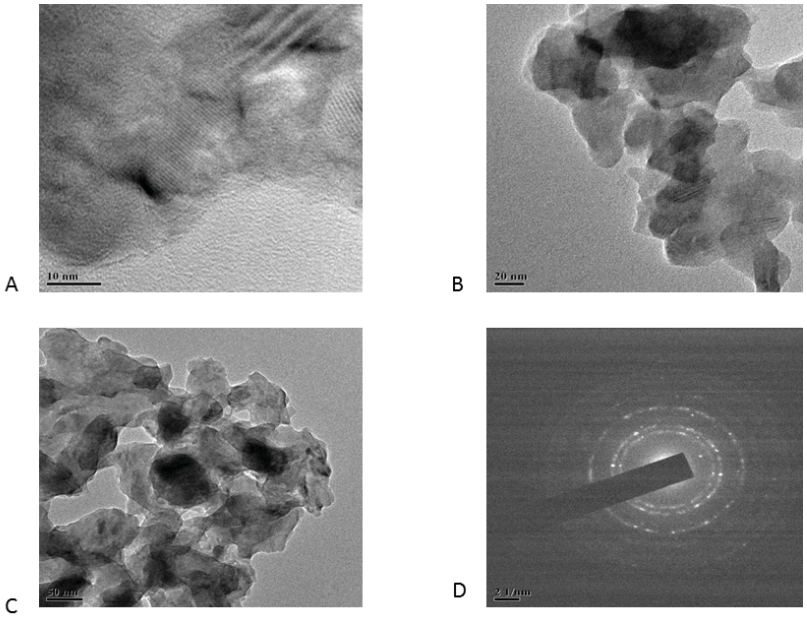

Fig. 7. A, B, and C are TEM images of $HA_{0.075}$ at various nanometer ranges and D is selected area electron diffraction (SAED) of HA nanoparticle

3. Conclusions

HA nanoparticle was successfully synthesized using green technology with culinary banana bract pectin. Pectin extracted from cell wall material of banana bract was characterized by ^{1}H NMR and FT-IR. The concentration of pectin is very crucial in the synthesis of nano hydroxyapatite. FT-IR analysis showed that pectin concentration plays significant role in improving purity of HA nanoparticle. Additionally, pectin concentration influenced crystallinity and size of synthesized HA nanoparticles, which were evidenced from XRD and SEM, respectively. The synthesized HA nanoparticles with 0.075% w/w of pectin concentration ($HA_{0.075}$) were found with discrete uniform shape and were highly pure with less crystallinity. TEM morphology of synthesized HA nanoparticles confirmed ceramic structure of HA nanoparticles with a size range of 20–50 nm. The synthesized nano HA has a great potential in biomedical fields, and more in depth characteristics assessment of these nanoparticles will bring more value addition.

References

Begum, Y.A. & Deka, S.C. (2017): Stability of spray dried microencapsulated anthocyanins extracted from culinary banana bract. *Int. J. Food Prop*. (DOI: 10.110.1080/10942912.2016.1277739).

Chatjigakis, A.K., Pappas, C., Proxenia, N., Kalantzi, O., Rodis, P. & Polissiou, M. (1998): FTIR spectroscopic determination of the degree of esterification of cell wall pectins from stored peaches and correlation to textural changes. *Carbohyd. Polym., 37*, 395–408.

Christensen, S.H. (1986): *Pectins.* -in: Glicksman, M. (Ed.) *Food hydrocolloids, Vol. III*., CRC Press, Boca Raton, Florida, pp. 206–227.

Dhanasekaran, D., Lawanya, S., Saha, S., Thajuddin, N. & Panneerselvam, A. (2011): Production of single cell protein from pine apple waste using yeast. *Innov. Rom. Food Biotechnol., 8*, 26–32.

Dorozhkin, S.V. & Epple, M. (2002): Biological and medical significance of calcium phosphates. *Angew. Chem. Int. Edit.*, *41*(17), 3130–3146.

Gilbert, P.U.P.A., Abrecht, M. & Frazer, B.H. (2005): The organic-mineral interface in biominerals. *Rev. Mineral Geochem. (RiMG), 59*, 157–185.

Gopi, D., Bhalaji, P.R., Prakash, V.C.A., Ramasamy, A.K., Kavitha, L. & Ferreira, J.M.F. (2010): An effective and facile synthesis of hydroxyapatite powders using oxalic acid ethylene glycol mixture. *Curr. Appl. Phys. 11*, 590–593.

Gopi, D., Govindaraju, K.M., Victor, C.A.P., Kavitha, L. & Rajendiran, N. (2008): Spectroscopic investigations of nano hydroxyapatite powders synthesized by conventional and ultrasonic coupled sol-gel routes. *Spectrochim. Acta A, 70*, 1243–1245.

Gopi, D., Kanimozhi, K., Bhuvaneshwari, N., Indira, J. & Kavitha, L. (2014): Novel banana peel pectin mediated green route for the synthesis of hydroxyapatite nanoparticles and their spectral characterization. *Spectrochim. Acta A*., *118*, 589–597.

Gopi, D., Kanimozhi, K. & Kavitha, L. (2015): *Opuntia ficus indica* peel derived pectin mediated hydroxyapatite nanoparticles: Synthesis, spectral characterization, biological and antimicrobial activities. *Spectrochim. Acta A, 141,* 135–143.

Hui, J., Zhang, X., Zhang, Z., Wang, S., Tao, L., Wei, Y. & Wang, X. (2012): Fluoridated HAp: Ln3þ (Ln ¼ Eu or Tb) nanoparticles for cell-imaging. *Nanoscale, 4*, 6967–6970.

Inbar, Y., Chen, Y. & Hadar, Y. (1989): Solid-state C-13 nuclear magnetic-resonance and infrared-spectroscopy of composted organic-matter. *Soil Sci. Soc. Am. J., 53*(6), 1695–1701.

Jamuna, J.B., Mahadevamma, S., Nandini, D.C. & Paramahans, V.S. (2012): Banana (*Musa* sp. var. *elakki bale*) flower and pseudostem: dietary fiber and associated antioxidant capacity. *J. Agr. Food Chem., 60*, 427−432.

Liu, L., Cao, J., Huang, J., Cai, Y. & Yao, J. (2010): Extraction of pectin with different degrees of esterification from mulberry branch bark. *Bioresource Technol., 101*, 3268–3273.

Maisara, S.M.A. & Pat, M.L. (2011): Synthesis and characterization of hydroxyapatite nanoparticles and β-TCP particles. *2nd International Conference on Biotechnology and Food Science IPCBEE,* IACSIT Press, Singapore. *7.*

Narayanan, K.B. & Sakthivel, N. (2010): Biological synthesis of metal nanoparticles by microbes. *Adv. Colloid Interfac., 156*(1-2), 1–13.

Preethi, P. & Balakrishnamurthy, G. (2011): Assessment of banana cultivars for pigment extraction from bracts, its suitability and stability as food colourant. *Int. J. Process Postharvest Technol. (IJPTI), 2*(2), 98–101.

Ranganna, S. (1986): *Handbook of analysis and quality control for fruits and vegetable products*. Tata McGraw-Hill Publishing Co. Ltd, New Delhi, pp. 40–42.

Rosenbohm, C., Lundt, I., Christensen, T.M.I.E. & Young, N.W.G. (2003): Chemically methylated and reduced pectins: Preparation, characterization by ^{1}H NMR spectroscopy, enzymatic degradation, and gelling properties. *Carbohyd. Res., 338*, 637–649.

Suchanek, W. & Yoshimura, M. (1998): Processing and properties of hydroxyapatite based biomaterials for use as hard tissue replacement implants. *J. Mater. Res., 13*, 94–117.

Tang, W., Yuan, Y., Liu, C., Wu, Y., Lu, X. & Qian, J. (2014): Differential cytotoxicity and particle action of hydroxyapatite nanoparticles in human cancer cells. *Nanomedicine-UK., 9*, 397–412.

Winning, H., Viereck, A., Norgaard, L., Larsen, J. & Engelsen, S.B. (2007): Quantification of the degree of blockiness in pectins using ^{1}H NMR spectroscopy and chemometrics. *Food Hydrocolloid., 21*, 256–266.

Wu, Q., Liu, C., Fan, L., Shi, J., Jia, H., Qi, Q., Sun, L. & Chen, F. (2013): Fabrication of heparinized hierarchically hollow hydroxyapatite microspheres as bone substitute for controlled growth factors delivery. *RSC Adv*., *3*, 7486–7494.

Yu, M., Zhou, K., Zhang, F. & Zhang, D. (2014): Porous HA microspheres as drug delivery: effects of porosity and pore structure on drug loading and in vitro release. *Ceram. Int., 40*, 12617–12621.

Zeng, J., Li, R., Liu, S. & Zhang, L. (2011): Fiber-like TiO_2 nanomaterials with different crystallinity phases fabricated via a green pathway. *ACS Appl. Mater. Inter.*, *3*, 2074–2079.

Zhang, X., Hui, J., Yang, B., Yang, Y., Fan, D., Liu, M., Tao, L. & Wei, Y. (2013): PEGylation of fluoridated hydroxyapatite (FAp):Ln3þ nanorods for cell imaging. *Polym. Chem.-UK., 4*, 4120–4125.